

Intervertebral Disc Implant

CHEMMAT 753 - Assignment 1

MARAH SHAHIN

May 7, 2020

Contents

1	Introduction	2
2	Background	2
2.1	Intervertebral Disc Degeneration	2
2.2	Treatments Methods for Intervertebral Disc Degeneration	3
2.2.1	Spine Fusion	3
2.2.2	Total Disc Replacement	3
3	Tissue Engineering	4
4	Scaffolds for Intervertebral Discs	5
4.1	Current Materials Used	5
5	Total Disc Replacement Implant	5
5.1	Materials being used	6
5.2	Requirements of an Ideal Implant	6
5.3	Influence to Biology	8
5.3.1	Long-term Factors	8
5.3.2	Healing	9
6	Materials Selection, CES Edupack	9
7	Methods used to make Scaffolds	10
8	Critical Analysis of Materials and Final Choice	10
8.1	Disc Component	10
8.2	Interface Plates	11
9	Design and Analysis of Prototype	12
9.1	Analysis of Designs	12
9.2	Final Design	13
9.2.1	Initial Stage of Sketches	13
9.2.2	Autodesk Inventor Stage	14
9.2.3	Stress Analysis	15
10	Conclusion	17
References		18
Appendix		22

1 Introduction

The purpose of this report is to investigate current implants used for intervertebral discs. From this investigation, a new prototype implant is designed that intends to address complications current discs encompass. The design for this implant draws from tissue engineering concepts and native disc properties. The material will be selected with the help of the CES Edupack software. Subsequently, a final model is presented with the ideal material composite and design ready to implement.

2 Background

Worldwide, back pain is the leading cause of disability. Approximately 80% of adults have said to experience lower back pain. Over 25% of people have encountered lower back pain in the past 3 months [1]. Back pain is associated with a number of risk factors such as: age, fitness level, pregnancy, weight gain and genetics [2].

Pain in the lower back is heavily related to intervertebral disc degeneration [3]. In short, this happens when the rubbery intervertebral discs in the spine lose their integrity from a natural aging process. Intervertebral discs provide height in a healthy back and allow the lower back to bend, stretch, and torsion. As the discs wear they lose their ability to cushion [1].

2.1 Intervertebral Disc Degeneration

The intervertebral disc (IVD) is made up of two distinct tissues: a thick centre, known as the nucleus pulposus (NP), and the outer annulus fibrosus (AF). The AF is encompassed by coaxial lamellae that construct its internal and external structure. This unique composition permits the IVD to impede movement when loads are large while also giving flexibility where loads are low. The AF parts are visible in figure 1 as the outer segment of 1a.

Where degeneration occurs, it is hard to recognize the two anatomical sections of the AF. In figure 1 the grooves of the annulus lamellae and absence of them are shown in 1a and 1b, respectively. The healthy disc has distinct clear grooves whereas, the degenerated disc has a smoothed over outer surface.

Experiments involving animal models show that extreme mechanical loading intensifies the degeneration of the disc. This indicates that IVD cells can detect and change with applied overloads to natural signals that follow tissue reactions [5, 6, 7, 8].

Degeneration also causes imbalances in the spine. The main changes during disc degeneration are presented in table 1.



Figure 1: a) Normal IVD , b) Degeneration of IVD. Sourced from [4]

Table 1: Disc Degeneration Changes. Sourced from [9]

Change	
Increases	Decreases
Matrix metalloproteinase production	pH
Progressive degeneration	Oxygen and nutrition
	Number of cells and their viability
	Extracellular matrix synthesis
	Disc integrity and thickness
	Overall functionality

Over a period of time, IVD degeneration can result in spinal stenosis, a cause for disability, significant pain and leg weakness in older people [4]. Thus, it is important to provide an effective and volatile treatment for IVD degeneration.

2.2 Treatments Methods for Intervertebral Disc Degeneration

Currently, the most popular methods are either noninvasive or invasive (surgery). Examples of noninvasive methods include: physical therapy and medication. Typical surgical methods include: spine fusion, total disc replacement (TDR) or regeneration, radiofrequency ablation and repair of the AF [10, 11]. The most common are spine fusion and TDR.

2.2.1 Spine Fusion

Spine fusion is the most popular method in treating IVD degeneration. IVD fusion removes the damaged disc to combine the upper and lower vertebral bodies (a large application in tissue engineering). This invasive technique uses a scaffold cage (shown in figure 2 and later discussed in section 4) to encourage bone growth between the two adjacent vertebrae. However, due to the newly fused bones, the patient loses mobility [11]. This lack of mobility introduces more issues in the long run. The combined bones means inadequate shock absorbance. In turn, this could lead to an additional IVD degeneration as the discs take on more force. Hence, another fusion surgery may be required. For this reason, only a limited number of spine fusion surgeries should be done on a patient [11].

2.2.2 Total Disc Replacement

This method removes the original degenerative disc and replaces it with a synthetic implant. Implants are either a ball-and-socket or one-piece design. TDR is often preferred over spine fusion due to the increased flexibility. Although, TDR comes with its own disadvantages. Ball-and-socket designs have issues with load and stress concentration, often due to hypermobility. One-piece implants attempt to solve these problems but are at greater risk to tears at the interface of materials or within. One-piece

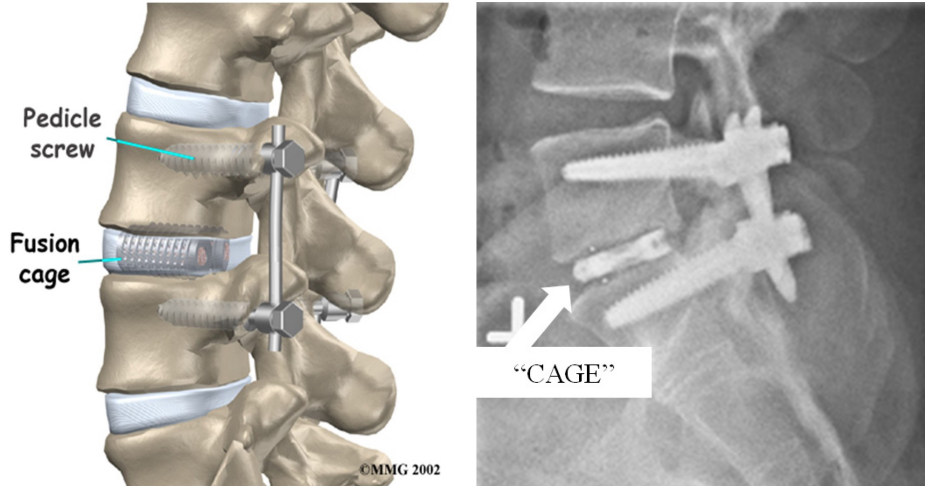


Figure 2: Scaffold Cage for IVD Fusion. Sourced from [11]

implants have been developed recently and thus, there are less studies regarding their performance. Overall both TDR system downfalls are caused by corrosion and wear [11].

3 Tissue Engineering

Tissue engineering couples the principles of materials and cell transplantation. The goal of tissue engineering is both to develop substitute tissue and promote endogenous regeneration [12]. The process involves manufacturing synthetic tissues from scaffolds, cells and biologically active molecules into practical functioning tissues to support damaged regions [13].

Tissue engineering depends on four fundamental aspects: the suitable cells for the job, a suitable environment (such as a scaffold), the correct biomolecules (such as growth factors to ensure the cells are healthy and productive) and mechanical and physical forces to promote cell development [13].

Tissue engineering is yet to reach its potential in current medical practice. Presently, engineered tissues have only taken the roles of bladders, cartilage and small arteries. Though, these surgeries are still at an experimental stage and expensive. Organs with a more complex nature (hearts, lungs and liver tissue) have been engineered in a lab but are far from ready for practice [13]. Despite complicated organs, tissue engineering has contributed various improvements to surgeries, such as scaffolds.

Although tissue engineering comes with its own set of challenges, with the development of biochemistry, stem cell biology, molecular biology, cell, genetic engineering and cloning fields, these issues are sure to mitigate in the near future.

Tissue engineers will be able to treat various diseases to a higher standard and improved success rate with the advancement of technology. Tissue engineering has already improved the lives of many patients with treated deformities, like those with intervertebral disc degeneration.

4 Scaffolds for Intervertebral Discs

A scaffold is a 3D structure implanted to promote tissue growth and regeneration. An example of a scaffold is the fusion cage in figure 2. Here, the scaffold is used to encourage bone graft to grow from one adjacent vertebral body, through the scaffold cage, to the next vertebral body (a large field in tissue engineering) [14]. Scaffolds have been engineered to influence the biological environment and support surrounding cells in producing their own extracellular matrix. The extracellular matrix acts as a structural mechanism by providing strength and a space for cellular attachment or storage for biomolecules. In some instances, a scaffold is implanted to simply enhance structural integrity [15]. Scaffolds can be developed from natural or artificial materials. Nature materials come from biological sources such as collagen, fibrin, alginate or ecellularized autogenic, meaning they're related to the cellular environment and give a lower chance of immunogenicity. Artificial materials are from synthetic sources such as polyglycolic acid and are able to be modified to better suit mechanical properties [13, 10].

4.1 Current Materials Used

Presently, the materials used for scaffold cage designs are the following [16]:

- cobalt-chromium alloy
- titanium (usually used as the interface)
- diamond-like carbon
- coatings
- ultrahigh-molecular-weight-polyethylene
- silicone
- polyurethane-polycarbonate elastomer

All these materials have a few significant features in common that allow them to be used in the body. First, they are all biocompatible. The body may reject the material if it's not biocompatible causing an intense inflammatory response and other severe reactions.

Second, they are all biodegradable otherwise cells will not be able to produce their extracellular matrix. Next, their mechanical properties mimic that of their intended anatomical site. While the body heals, the scaffold must be strong enough to function as the supporting system [17].

These three factors are only part of the requirements needed to ensure success for any scaffold.

5 Total Disc Replacement Implant

Spine fusion is a classical method that only partially solves IVD degeneration. The surgery does not restore functionality or mobility. Spinal fusion clinical success rates are also low [18].

Due to these limitations, a TDR implant is developed instead of a fusion cage. TDR may be a promising

method for the future. These implants are more complicated and hold their own problems. Nevertheless, the implants have the potential to provide the mobility and functionality one had prior to disc degeneration.

The development process started with materials then structural design. The artificial one-piece device is designed based on the properties of a native disc and implants currently being used. The goal is to minimise risks and maximise functionality.

An IVD implant can be viewed as a threefold structure. First, the inner disc, intended to mimic the NP. Second, the outer disc or, AF of the implant. Lastly, the interface plates. These lay between the disc implant and the bone. The plates must be sturdily attached to the bone.

The development and design of an IVD replacement requires careful consideration and research. There are already a variety of designs for these implants on the market; some of which have also been approved to be used in practice. These are further discussed below.

5.1 Materials being used

Table 2 shows examples of current disc replacements being used and their respective attributes.

It is noted there are many common biomaterials across all classifications and bearing designs. This suggests these biomaterials have mechanical properties similar to that of a native disc. Furthermore, all the one-piece devices have elastomer cores with titanium plates; indicating the combination of the two replicates the function of an IVD or close to it.

5.2 Requirements of an Ideal Implant

An ideal scaffold would be a replica of an intervertebral disc as this would possess all the mechanical and biological properties required. The replica would be both accepted by the body and effective. Therefore, the ideal scaffold can be described by the nature of an original IVD. The optimal material and design would be the closest to this classification. Table 3 illustrates the relevant properties of a healthy IVD. An overall structure that biologically mimics that of IVD is also important. Thus, having a separate lamella outer with an inner nucleus-like design would increase the likelihood of success.

Additional requirements are listed below [10]:

1. Porous to ensure no restriction on tissue growth. Also to allow diffusion of nutrients and waste and to enable cellular communication (mainly related to surface of plates).
2. Allow possible cell proliferation, differentiation and attachment.
3. Shape and size must fit where implantation is intended.

Device	Classification	Biomaterials	Bearing Design	Examples of Manufacturer
CHARITE	MoP	CoCr-UHMWPE	Mobile	DePuy Spine
Prodisc-L	MoP	CoCr-UHMWPE	Fixed	DePuy Synthes
Activ-L	MoP	CoCr-UHMWPE	Mobile	Aesculap
Mobidisc	MoP	CoCr-UHMWPE	Mobile	LDR Medical
Baguera	MoP	DLC coated Ti-UHMWPE	Fixed	Spineart
NuBlac	PoP	PEEK-PEEK	Fixed	Pioneer
Maverick	MoM	CoCr-CoCr	Fixed	Medtronic
Kineflex	MoM	CoCr-CoCr	Mobile	SpinalMotion
Flexicore	MoM	CoCr-CoCr	Constrained	Stryker
XL-TDR	MoM	CoCr-CoCr	Fixed	NuVasive
CAdisc-L	1P	PU-PC graduated modulus	1P	Rainier Technology
Freedom	1P	Ti plates; silicone PU-PC core	1P	Axiomed
eDisc	1P	Ti plates, elastomer core	1P	Theken
Physio-L	1P	Ti plates, elastomer core	1P	NexGen Spine
M6-L	1P	Ti plates; PU-PC core with UHMWPE fiber encapsulation	1P	Spinal Kinetics
LP-ESP (elastic spine pad)	1P	Ti endplates; PU-PC coated silicone gel with microvoids	1P	FH Orthopedics

CoCr—Cobalt-chromium alloy. UHMWPE—Ultra-high molecular weight polyethylene. DLC—Diamond-like carbon. Ti—Titanium. PEEK—Polyether ether ketone. PU-PC—Polyurethane-polycarbonate elastomer.

Table 2: Summary of current total disc replacement types

Sourced from [11] MoP=metal on polymer, PoP=polymer on polymer, MoM=metal on metal, 1P=one-piece, Fixed=no moving parts except sliding socket over ball, Mobile, Constrained=motion of ball permitted.

Intact			
Compressive modulus (MPa)			
ND	10–20		
D	5–12		
—	4–25		
Tension modulus (MPa)			
ND	2.6–3.5		
—	n/a		
Bending stiffness (N × mm/deg)			
Flexion	500–2200		
Extension	1100–2500		
Lateral	1800–3800		
Torsional stiffness (N × mm/deg)			
ND	700–1100		
D	600–1800		
Shear stiffness (N/mm)			
Lateral	40–300		
Anterior-posterior	20–300		
		Property	Nucleus (Human)
		Major Diameter (mm)	35
		Minor Diameter (mm)	25
		Height (mm)	13
		Specific Heat (Nmm/kg/°C)	3e6
		Density(kg/mm ³)	1.09e-6
		Conductivity(N/sec/°C)	1.472
			1.008

Table 3: Mechanical, Geometry and Material Properties of an Intact Human IVD
ND=nondegenerate, D=degenerate. Sourced from [19, 20]

A 2006 study [21] indicates that an ideal tissue-engineered IVD will likely have a 5–10 MPa range modulus and a failure strength greater than 1.67 MPa. Implanted scaffolds with these properties can then achieve

the objective loading stress and restore disc height.

5.3 Influence to Biology

All implants, including IVD discs, affect surrounding biology in some way. There will be both immediate and long term reactions. Initially, the surgical invasion causes surrounding blood vessels to increase wall permeability with fluid leakage into tissues and recruitment of polymorphonuclear leucocytes into the affected area. Also passive red blood cell leakage occurs; this is acute inflammation. The inflammation is accompanied by the recruitment of circulatory monocytes. Such cells grow into macrophages as they reach the tissue where they swallow and extract dead and foreign material. Fibroblasts are further recruited and new blood vessels are generated, resulting in a young fibrous tissue called granulation. Connective tissue cells, i.e. chondrocytes, osteoblasts and fibroblasts, come from the same progenitor cell, and fibrous tissue, bone or cartilage that develop in the bone healing content based on the local environments [22]. In the course of time the implant relieves pressure on compressed nerves [23]. The inevitable acute inflammatory response fades away after a few days. Further reactions include: potential immune reactions to implant and lack of nutritional supply. There was also shown to be an increase in extracellular matrix production and cell proliferation [24]. Additionally, the tissue engineered IVD engrafted to the host tissue eventually [25].

5.3.1 Long-term Factors

The factors that affect the long-term response at the bone-implant interface include the material's modulus, surface roughness and porosity, and chemistry. TDR implants specifically have a reoccurring issue of wear debris. The biological response to such material is due to particle shape, particle size, particle number and debris chemical composition. Therefore, the host's reaction is dependent on both the design of the replacement and its material.

Reactions independent of material include osteolysis and inflammation. Osteolysis is a degradation mode which involves bone destruction. Osteolysis in TDR implants is induced predominantly by implant micro-movements and the biological reaction to wear debris.

Bone growth and maintenance are the products of the resorption equilibrium responses induced by osteoblasts and osteoclasts, respectively. Debris particles disrupt bone homeostasis via an inflammatory response. In turn, this stimulates osteoclasts to mature and increase bone resorption. The mixture of such wear processes lead to higher wear levels over time as the resorption loosens the system, allowing more space for movement and debris causing osteolysis. This may not be the case for MoM implants however, it has been suggested that wear rates are lower for such implants [16].

5.3.2 Healing

The bone fracture made by the insertion of the implant eventually repairs. Fibrous tissue and new bone is produced when the implant is fixed. This leads to the formation of a callus which is at first, swelling of the bone but later remodeling. Dead bone fragments are removed by osteoclasts. The fragments also may serve as a scaffold for new bone to be deposited. The bone grows upright to the surface of the titanium plates [22]. With time, the bone will closely fit the implant profile.

6 Materials Selection, CES Edupack

To develop a prototype of the TDR disc section of the implant the CES Edupack software was used to narrow the available database (level 3 bioengineering database) of materials down to three viable options. The following restrictions were placed are shown in table 4.

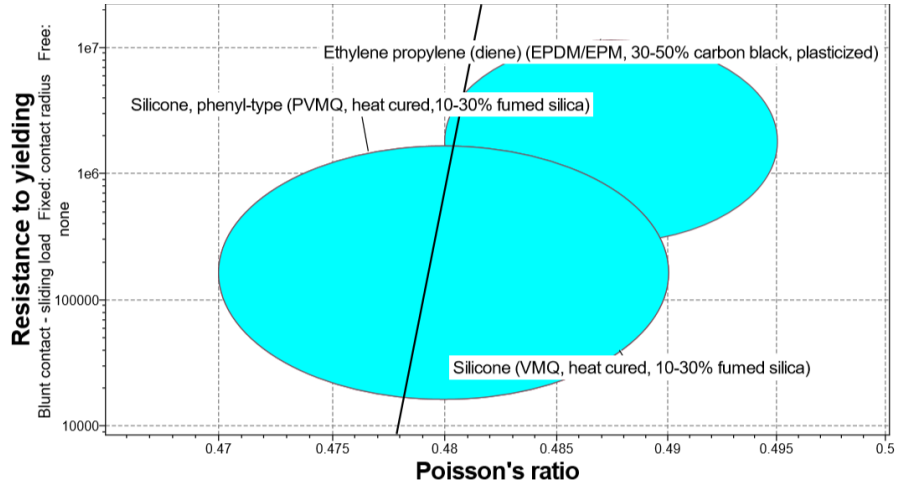
Property	limit		Ref
	min	max	
Young's Modulus MPa	5	10	[21]
Tensile Strength MPa	1.67	-	[21]
Biomedical Materials		Yes	[17]
Density kg/m^3	1035.5	1176	[20]
Shear Modulus MPa	2	9	[26]
Poisson's Ratio	0.02	0.48	[27]

Table 4: Limitations placed on materials for selection

The restrictions in table 4 were inspired by and drew knowledge from the "Requirements of an Ideal Implant" (section 5.2). The properties were deemed to be the most significant due to the required strength needed for the job. The material also needed to be "biomedical" so the body does not reject it. The literature indicated young's modulus was of the upmost importance [28]. These limitations left four materials that fit the criteria. To further narrow the options, a graph was created to show the material's resistance to yielding against Poisson's ratio.

The yielding test involves abrasion by blunt contact which is promoted by onset of yielding. In essence, load is applied normal and tangential to the flat plate. The type of force experienced in this simulation is the same that the disc will experience in its implantation site. Therefore, high performance in this test was considered an important factor. The Poisson's ratio is also examined to ensure the material's value is as close to that of a native disc as possible, since the estimated value of 0.22 is unattainable. The line shown in figure 3 presents the importance of each factor; high importance on performance and less on Possion's ratio. Possion's ratio varies very little regardless of the material so it is not the highest priority. The top three materials left were: ethylene propylene (EPDM/EPM), silicone phenyl-type(PVMQ) and silicone (VMQ). All three of which are elastomers.

Figure 3: Resistance to yielding vs. Poisson's ratio



7 Methods used to make Scaffolds

The electrospinning method is common in the production of fiber and by extension, these implants [29]. The method applies a strong electric field on the polymer which generates nanoscale fibers. The end result mimics the extracellular matrix component closely, making this a technique of interest for the production of IVD implants [30].

Where titanium is involved, the implant is often cast then fixturing is usually needed to ensure the device is near perfect (as they often have to be). Due to the complex and precise nature of these implants, new techniques have risen in the manufacturing field. For instance, newly developed machines with 12-axes of motion enables full positioning capability in any space. These machines also provide a close tolerance for fine details [31].

Micromolding is also an interesting, recently developed technique. This process allows for the manufacture of medical parts to an accuracy as fine as 0.0001 cu. in. There are many other advancements that shed hope for the development and future of TDR implants [31].

Many manufacturing methods are used for thermosetting materials, in general and in particular for silicone elastomers, including casting, extrusion and molding. The specific manufacturing activity depends on the viscosity of the material to be used and the form and structure of the end product [32].

8 Critical Analysis of Materials and Final Choice

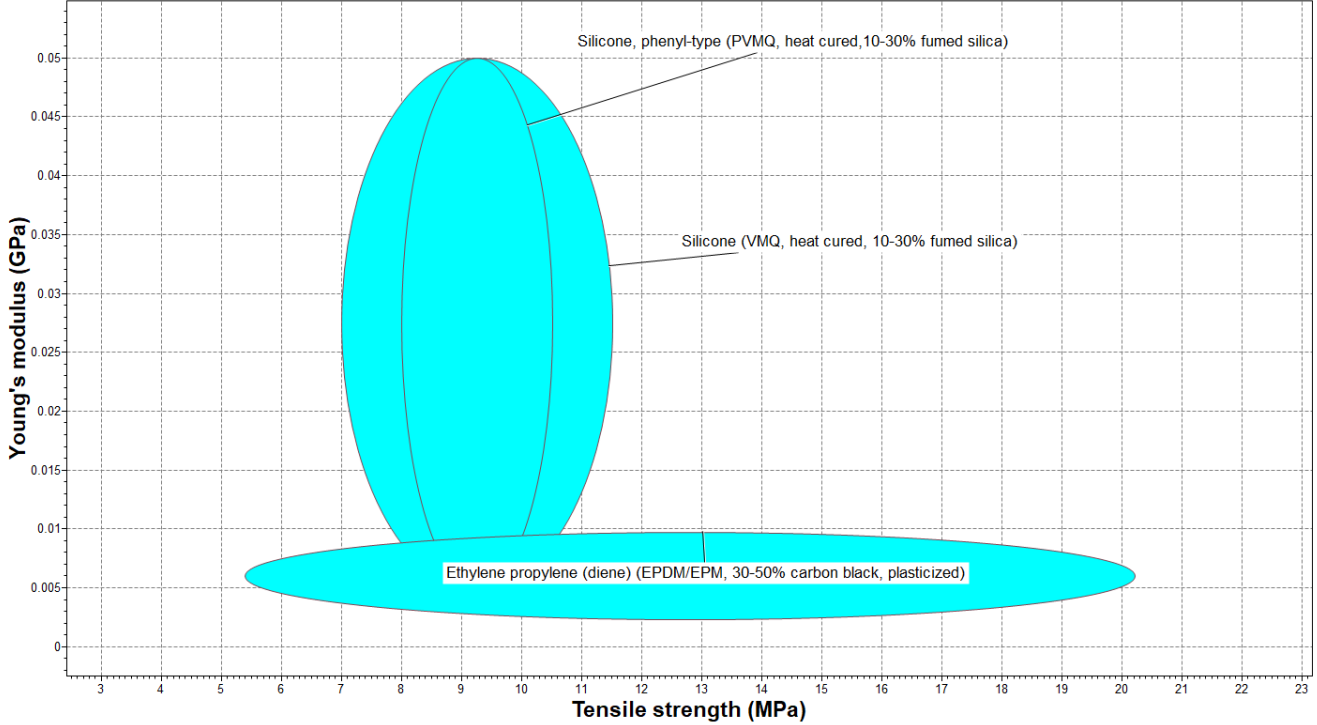
8.1 Disc Component

Firstly, it is noted all three materials do not biodegrade which is necessary for the disc.

A problem with current IVD replacements is that they do not deal well with compressive forces. To address this issue, two separate materials will be used for the disc segment of the implant. To achieve a similar mechanical response to that of a native disc, the implant would require a low modulus core and

surrounding higher modulus material [28].

Figure 4: Young's Modulus vs. Tensile Strength



From the three materials, figure 4 shows EPDM/EPM to have the lowest modulus value and therefore will be used as the implant NP.

VMQ and PVMQ have extremely similar qualities. The main differences are price and thermal properties. VMQ is much cheaper than PVMQ with average prices of \$8 and \$28 per kg, respectively. PVMQ is flexible at low temperatures whereas VMQ holds its flexibility at a large range of temperatures (-50 to 200°C). Additionally, a limitation of PVMQ is strength (no temperature specified). VMQ has a limitation of "low temperature strength" rather than strength in general. Higher temperature flexibility and strength are preferred because regular body temperature is approximately 37°C [33].

Given VMQ is much cheaper and performs better over a larger range of temperatures, it will be used for the AF of the disc.

8.2 Interface Plates

A similar material selection process could have been adopted for the plates used at the interface of the bone and artificial disc. However, the literature and current implants suggest cobalt-chromium alloy (CoCr) and titanium (Ti) are both strong candidates for the role. The material used for the interface plates from the implants in table 2 were either CoCr or Ti. Ti was shown to be less problematic with debris later in the healing stage [28]. More importantly, Ti has a closer young's modulus value to that

of cortical bone (which is what it will be mimicking) [34]. Although, Ti is typically more expensive, it will result in an overall biologically superior and safer implant for the patient and thus will be used as the plates.

Finally the surface of the plates is also important as they are the direct interface to cortical bone. Having a porous surface coating of the metal implant is an effective strategy for enhancing incorporation into the bone (mentioned in subsection 5.3). This surface has been used in previous designs in the form of beads or intertwined wire-like structure. Studies have shown this coating is favourable and pore size is not too relevant. Results also found fire mesh is superior to beads [22].

9 Design and Analysis of Prototype

9.1 Analysis of Designs

Three implants, all with elastomeric cores, were of most interest during the design process. The designs have been shown to work well in the past but still can be improved. In designing a new implant, the designs were compared and contrasted to determine the best features and where the part could be revised.

Figure 5: Physio-L Artificial Disc Extracted from [28]



Firstly, much inspiration came from the Physio-L implant shown in figure 5. The hourglass shape helps relieve stress at the core and ends of the disc however, this also may cause issues of hypermobility (discussed in subsection 2.2.2). The surface beads covering a large area is a strength for the device, this means the bone will bind to the implant well. The way the implant will attach (line on surface that fractures bone) may not provide enough structural integrity before binding occurs.

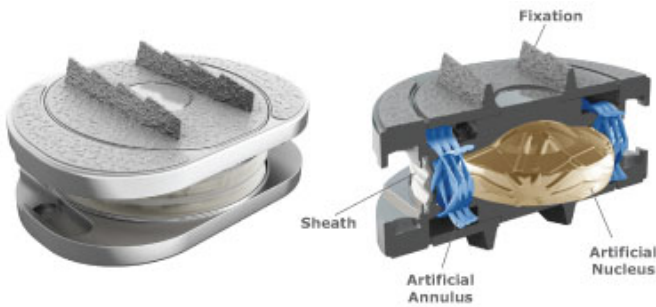


Figure 6: M6-L
Extracted from [35]

Next, the M6-L device shown in figure 6. Although the interior isn't that of a traditional TDR implant, it does provide for an unparalleled effective result. This implant's unique structure gives rise to an almost identical quality of motion as an intact disc. The downside to this design is that it may not provide the same flexibility as that of a native disc. The cage-like AF section is the gray parts surrounding the NP (tan section) and may be restricting movement. The surface of the fixation is also coated with titanium plasma spray for osseointegration. The spikes for fracture also appear to be able to hold stronger than the Physio-L.

Figure 7: The Freedom Lumbar Disc



Extracted from [28]

Lastly, the Freedom Lumbar Disc in figure 7. The pyramid spikes ensure a sturdy bond between the bone and plates. The porous surface also aids in the osseointegration process. However the core, being one material does not comprehensively replicate the mechanical properties of a native implant but still has desirable viscoelastic properties [28].

9.2 Final Design

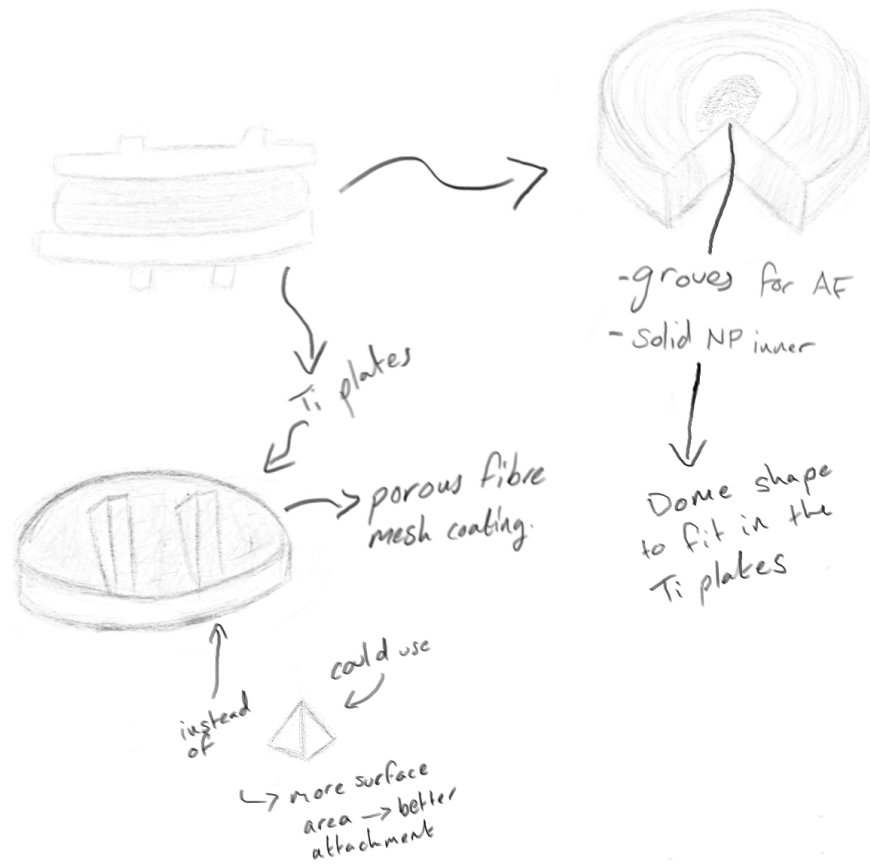
The overall implant design was based on current devices and possible improvements. The materials will be manufactured using electrospinning for the elastomer AF, casting & fixturing for Ti plates and casting, extrusion & molding for the elastomer NP. Initially only sketches were designed to visualise concepts and important attributes. Next, with a reflection on required dimensions, the parts were constructed on Autodesk Inventor and assembled. The model can later be 3D printed.

Finally, a stress analysis was conducted on the implant to estimate performance.

9.2.1 Initial Stage of Sketches

First ideas of how the prototype might look are shown in figure 8.

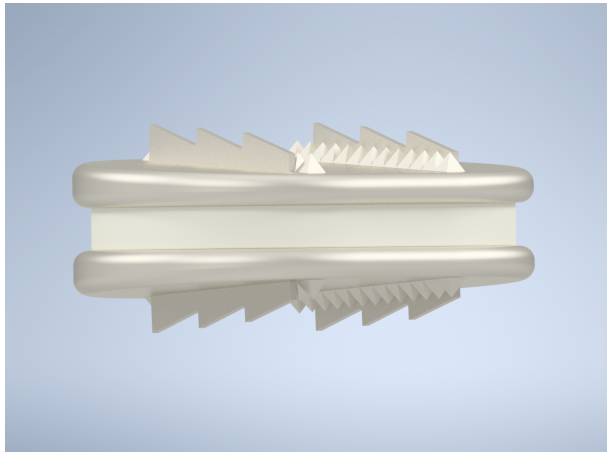
Figure 8: Initial Sketch Ideas



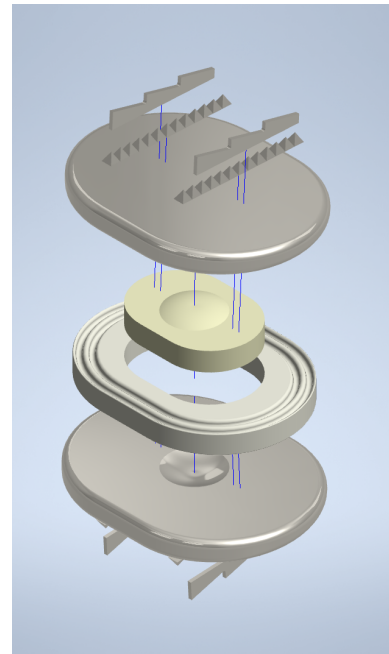
The concept included a few features from the implants mentioned with small improvements. The surface plates will include multiple points of fracture to maximise surface area for osseointegration and easier migration. The multiple points also means in the first few weeks of implantation, the implant will be firm and securely placed in its site. The plate will also be coated in fibre mesh as that was found to be the most effective for the bone to grow onto. The core will have two separate parts to mimic the AF and NP. The AF will be a fibrous structure and will have a slightly larger young's modulus.

9.2.2 Autodesk Inventor Stage

After the sketches were examined, the geometric properties from table 3 were taken into consideration to build the computer-aided design. The final result is shown in figure 9.



(a) Side View



(b) Exploded View

Figure 9: Final Desgin

The first part developed was the artificial NP (the middle yellow section). The part has dome shape top and bottom to increase stability of the structure. The next constructed part was the AF. The structure should be fibrous in nature to better support the spine. However, the AF should also ease into a more solid implant until it meets the NP. The Ti plates were designed with a small incline to fit the lordosis angle. Full details of dimensions and additional views can be found in the appendix. The plates also have an identical dome cut out to fit that on the NP. Finally, the features on the plate were created to combine aspects from both the M-6 and the Freedom Lumbar Disc. It is also noted a physical model will also have fire mesh lined on any interface surface; this could not be represented on Inventor.

9.2.3 Stress Analysis

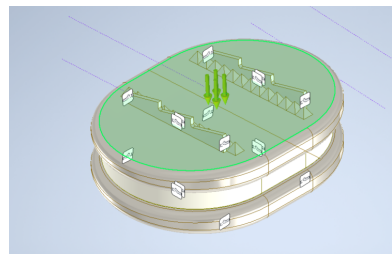
To validate the implant a stress analysis was carried out. The applied pressure was that a normal disc would experience. The load these discs experience is approximately 1.2 times the body weight [36]. The average mass of a human being was found to be 62kg [37]. By assuming the shape of the implant surface

to be an ellipse, the pressure to apply was calculated as follows:

$$\begin{aligned}
 Pressure &= \frac{Force}{Area} \\
 Force &= 62\text{kg} \cdot 9.81\text{m/s}^2 \cdot 1.2 \\
 Area &= rad_{long} \cdot rad_{short} \cdot \pi \\
 Area &= 0.0325\text{m} \cdot 0.025\text{m} \cdot \pi \\
 Pressure &= \frac{729.86\text{N}}{0.003\text{m}^2} \\
 &\approx 0.24\text{MPa}
 \end{aligned} \tag{1}$$

The pressure was applied on the surface of the plate as shown in figure 10.

Figure 10: Location of Pressure Applied

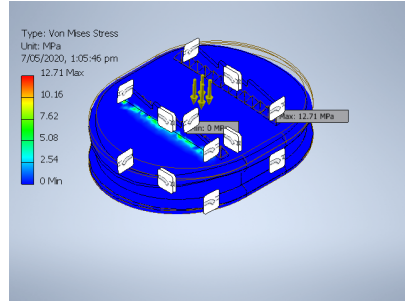


Constraints are also slightly visible in figure 10. Sides of the bone fixtures were assumed to be fixed as this was believed to best replicate the situation in the spine.

The most significant results examined were the strains. Strains from the load should not exceed 15% in the disc [36]. The strain results show there was no more than 0.038% strain in any direction or location throughout the implant. The next important factor considered was areas of high stress points. Figure 11 shows the stresses are mostly well distributed with small areas of high stress. This stress however, is not extremely large and therefore, not concerning.

To ensure the analysis is comprehensive, the maximum load a disc experiences was also observed. Thus, a second stress analysis with all the same components as the first, except a force of 3000N (max, [38]) was applied. The largest strain in this situation was 0.3%. The full summary can be found in the appendix.

Figure 11: High Stress Points



Another notable result was displacement did not exceed 0.002mm on the edges. Figures and a summary further illustrating these results can be found in the appendix. Overall, the implant was found to be structurally sound for its expected use.

10 Conclusion

Ultimately, a thorough analysis of literature shows treatments for IVD degeneration is a growing field. Treatments have not been perfected and sometimes issues cannot be identified immediately (osteolysis). Future implants are not only building on current ones but also attempting to branch into experimental new designs. The higher risk of less certainty may yield for a high reward of mitigated issues.

In developing a treatment for IVD degeneration, the least problematic design was taken and improved upon. The one-piece TDR implant is predicted to perform better than competitors. The implant figure is halfway between an hourglass shape and flat shape to provide mobility without the risk of hypermobility. The fine mesh coated surface gives superior osseointegration. A prototype model was designed on Autodesk Inventor where a stress analysis could be simulated. The prototype can also be 3D printed to better inspect features and faults. Progression in the design process (real life stress analysis) will highlight the implant's flaws.

It is clear with the growth of the tissue engineering, higher quality implants will be developed as the problem becomes more deeply understood. Until then, designs such as the one outlined in this report can attempt to address IVD degeneration.

References

- [1] Low Back Pain Fact Sheet | National Institute of Neurological Disorders and Stroke, . URL <https://www.ninds.nih.gov/Disorders/Patient-Caregiver-Education/Fact-Sheets/Low-Back-Pain-Fact-Sheet>.
- [2] Back pain - Symptoms and causes, . URL <https://www.mayoclinic.org/diseases-conditions/back-pain/symptoms-causes/syc-20369906>. Library Catalog: www.mayoclinic.org.
- [3] Maurits W van Tulder, Bart W Koes, and Lex M Bouter. A cost-of-illness study of back pain in the netherlands. *Pain*, 62(2):233–240, 1995.
- [4] Jill PG Urban and Sally Roberts. Degeneration of the intervertebral disc. *Arthritis Research & Therapy*, 5(3):120–130, 2003. ISSN 1478-6354. doi: 10.1186/ar629. URL <https://www.ncbi.nlm.nih.gov/pmc/articles/PMC165040/>.
- [5] TAPIO Videman, MARKKU Nurminen, and JD Troup. 1990 volvo award in clinical sciences. lumbar spinal pathology in cadaveric material in relation to history of back pain, occupation, and physical loading. *Spine*, 15(8):728–740, 1990.
- [6] Jeffrey C Lotz, Olivier K Colliou, Jennie R Chin, Neil A Duncan, and Ellen Liebenberg. Compression-induced degeneration of the intervertebral disc: an in vivo mouse model and finite-element study. *Spine*, 23(23):2493–2506, 1998.
- [7] Michael A Adams and Patricia Dolan. Could sudden increases in physical activity cause degeneration of intervertebral discs? *The Lancet*, 350(9079):734–735, 1997.
- [8] Jeffrey C Lotz and Jennie R Chin. Intervertebral disc cell death is dependent on the magnitude and duration of spinal loading. *Spine*, 25(12):1477–1483, 2000.
- [9] Sibylle Grad, Mauro Alini, David Eglin, Daisuke Sakai, Joji Mochida, Sunil Mahor, Estelle Collin, Biraja Dash, and Abhay Pandit. Cells and biomaterials for intervertebral disc regeneration. *Synthesis lectures on tissue engineering*, 5(1):1–104, 2010.
- [10] N. S. Kalson, S. Richardson, and J. A. Hoyland. Strategies for regeneration of the intervertebral disc. *Regenerative Medicine*, 3(5):717–29, 09 2008. URL <http://ezproxy.auckland.ac.nz/login?url=https://search-proquest-com.ezproxy.auckland.ac.nz/docview/881677140/accountid=8424>. Copyright - © 2008 © Future Medicine Ltd; Last updated - 2014-03-20.
- [11] Brody A Frost, Sandra Camarero-Espinosa, and E Johan Foster. Materials for the spine: anatomy, problems, and solutions. *Materials*, 12(2):253, 2019.

- [12] Robert Lanza, Robert Langer, and Joseph Vacanti, editors. *Principles of Tissue Engineering*. Elsevier, 4th edition, 2014. ISBN 978-0-12-398358-9. doi: 10.1016/C2011-0-07193-4. URL <https://linkinghub.elsevier.com/retrieve/pii/C20110071934>.
- [13] *Tissue Engineering and Regenerative Medicine*, . URL <https://www.nibib.nih.gov/science-education/science-topics/tissue-engineering-and-regenerative-medicine>.
- [14] Peter Ullrich MD. Interbody Cages for Spine Fusion. URL <https://www.spine-health.com/treatment/spinal-fusion/interbody-cages-spine-fusion>. Library Catalog: www.spine-health.com.
- [15] Daniel Howard, Lee D Butterly, Kevin M Shakesheff, and Scott J Roberts. Tissue engineering: strategies, stem cells and scaffolds. *Journal of Anatomy*, 213(1):66–72, July 2008. ISSN 0021-8782. doi: 10.1111/j.1469-7580.2008.00878.x. URL <https://www.ncbi.nlm.nih.gov/pmc/articles/PMC2475566/>.
- [16] John Reeks and Hong Liang. Materials and their failure mechanisms in total disc replacement. *Lubricants*, 3(2):346–364, 2015.
- [17] Fergal J O'brien. Biomaterials & scaffolds for tissue engineering. *Materials today*, 14(3):88–95, 2011.
- [18] Benjamin Whatley. Biofabrication of scaffolds for intervertebral disc (ivd) tissue regeneration. 2013.
- [19] Grace O'Connell, J. Leach, and Eric Klineberg. Tissue engineering a biological repair strategy for lumbar disc herniation. *BioResearch Open Access*, 4:431–445, 11 2015. doi: 10.1089/biores.2015.0034.
- [20] Gye-Rae Tack, Jin Seung Choi, Bongsoo Lee, Beobyi Lee, Soon-Cheol Chung, and yi Han. A study on the factors affecting the temperature distribution within intervertebral disc during electrothermal therapy. pages 63–66, 01 2006.
- [21] Jun Yao, Sergio R Turteltaub, and Paul Ducheyne. A three-dimensional nonlinear finite element analysis of the mechanical behavior of tissue engineered intervertebral discs under complex loads. *Biomaterials*, 27(3):377–387, 2006.
- [22] L. Ambrosio and E. Tanner. *Biomaterials for Spinal Surgery*. Woodhead Publishing Series in Biomaterials. Elsevier Science, 2012. ISBN 9780857096197. URL <https://books.google.co.nz/books?id=Yc9ZAgAAQBAJ>.
- [23] ViewMedica / Swarm Interactive. Total Disc Replacement Back Surgery Video. URL <https://www.spine-health.com/video/total-disc-replacement-back-surgery-video>.

- [24] Yu Moriguchi, R Navarro, P Grunert, J Mojica, K Hudson, T Khair, M Alimi, L Bonassar, and R Hartl. Total disc replacement using tissue engineered intervertebral discs in an in-vivo beagle model. *PLoS One*, 12(10):1–18, 2017.
- [25] James Dowdell, Mark Erwin, Theodoe Choma, Alexander Vaccaro, James Iatridis, and Samuel K. Cho. Intervertebral disk degeneration and repair. *Neurosurgery*, 80(3):S46–S54, 03 2017. URL <http://ezproxy.auckland.ac.nz/login?url=https://search-proquest-com.ezproxy.auckland.ac.nz/docview/1969978150?accountid=8424>. Copyright - Copyright © 2016 Congress of Neurological Surgeons; Last updated - 2018-01-09.
- [26] Nandan L Nerurkar, Dawn M Elliott, and Robert L Mauck. Mechanical design criteria for intervertebral disc tissue engineering. *Journal of biomechanics*, 43(6):1017–1030, 2010.
- [27] Kinda Khalaf, Mohammad Nikkhoo, Ya-Wen Kuo, Yu-Chun Hsu, Mohammad Parnianpour, Naira Campbell-Kyureghyan, Mohammad Haghpanahi, and Jaw-Lin Wang. Recovering the mechanical properties of denatured intervertebral discs through platelet-rich plasma therapy. In *2015 37th Annual International Conference of the IEEE Engineering in Medicine and Biology Society (EMBC)*, pages 933–936. IEEE, 2015.
- [28] Daniel H Kim, Dilip K Sengupta, Frank P Cammisa, and Richard G Fessler. *Dynamic reconstruction of the spine*. Thieme Stuttgart, 2015.
- [29] Leon J Nesti, Wan-Ju Li, Rabie M Shanti, Yi Jen Jiang, Wesley Jackson, Brett A Freedman, Timothy R Kuklo, Jeffrey R Giuliani, and Rocky S Tuan. Intervertebral disc tissue engineering using a novel hyaluronic acid–nanofibrous scaffold (hanfs) amalgam. *Tissue Engineering Part A*, 14(9):1527–1537, 2008.
- [30] Nandana Bhardwaj and Subhas C Kundu. Electrospinning: a fascinating fiber fabrication technique. *Biotechnology advances*, 28(3):325–347, 2010.
- [31] Machining Titanium Implants, August 2006. URL <https://www.americanmachinist.com/machining-cutting/article/21893863/machining-titanium-implants>. Library Catalog: www.americanmachinist.com.
- [32] AD Padsalgikar. 3-speciality plastics in cardiovascular applications. *Plastics in Medical Devices for Cardiovascular Applications: William Andrew Publishing*, pages 53–82, 2017.
- [33] What Is the Normal Body Temperature: Babies, Kids, Adults, and More, . URL <https://www.healthline.com/health/what-is-normal-body-temperature>. Library Catalog: www.healthline.com.
- [34] Yang Li, Guy R Fogel, Zhenhua Liao, and Weiqiang Liu. Finite element model predicts the biomechanical performance of cervical disc replacement and fusion hybrid surgery with various geometry

of ball-and-socket artificial disc. *International journal of computer assisted radiology and surgery*, 12(8):1399–1409, 2017.

- [35] M6-L Overview | Spinal Kinetics, . URL <http://www.spinalkinetics.com/m6-l/m6-l-overview/>. Library Catalog: www.spinalkinetics.com.
- [36] Rajib K Shaha, Daniel R Merkel, Mitchell P Anderson, Emily J Devereaux, Ravi R Patel, Amir H Torbati, Nick Willett, Christopher M Yakacki, and Carl P Frick. Biocompatible liquid-crystal elastomers mimic the intervertebral disc. *Journal of the Mechanical Behavior of Biomedical Materials*, page 103757, 2020.
- [37] Sarah Catherine Walpole, David Prieto-Merino, Phil Edwards, John Cleland, Gretchen Stevens, and Ian Roberts. The weight of nations: an estimation of adult human biomass. *BMC public health*, 12(1):439, 2012.
- [38] Hendrik Schmidt, Kim Häußler, Hans-Joachim Wilke, and Uwe Wolfram. Structural behavior of human lumbar intervertebral disc under direct shear. *Journal of applied biomaterials & functional materials*, 13(1):66–71, 2015.

Appendix

Figure 12: Exploded Drawing

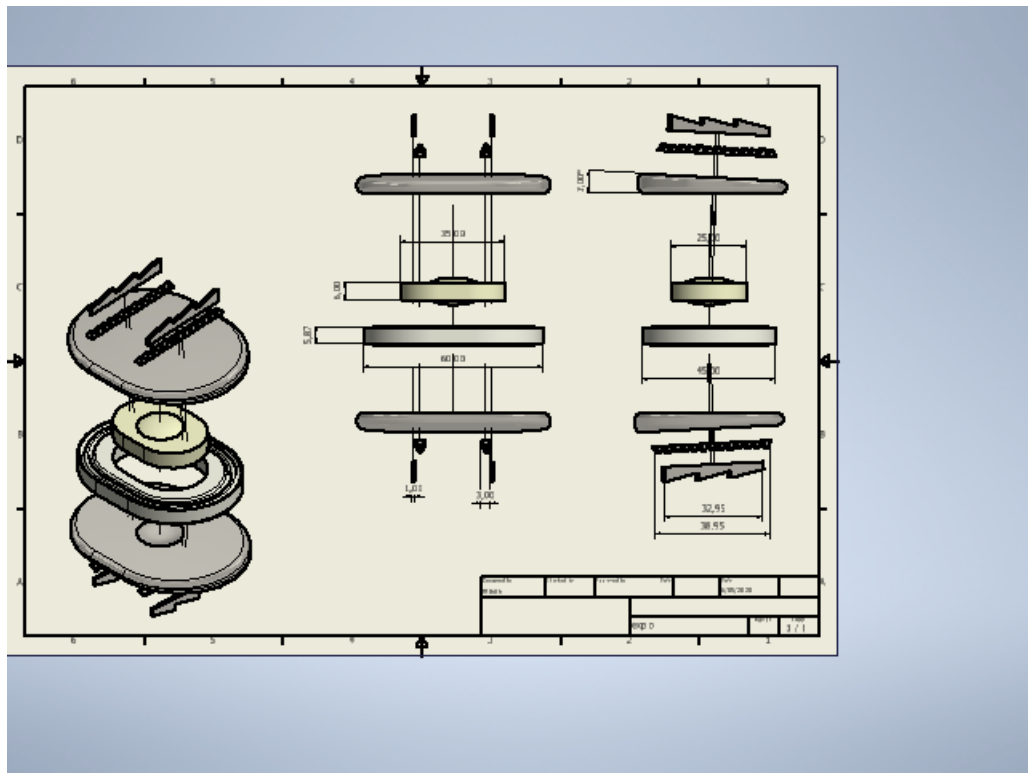


Figure 13: Full Drawing

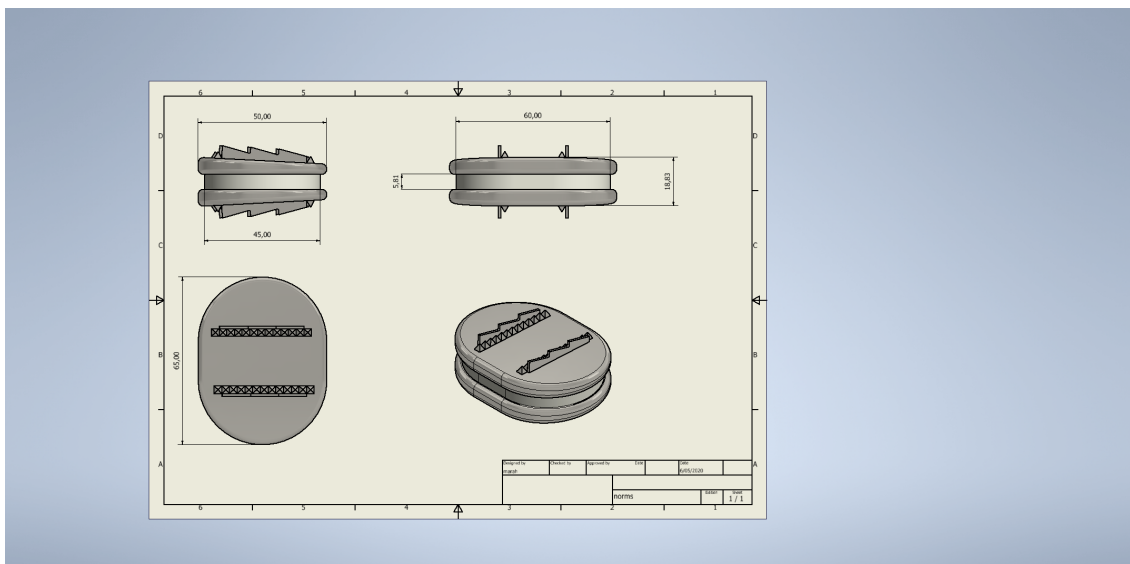


Figure 14: Exploded Bottom View

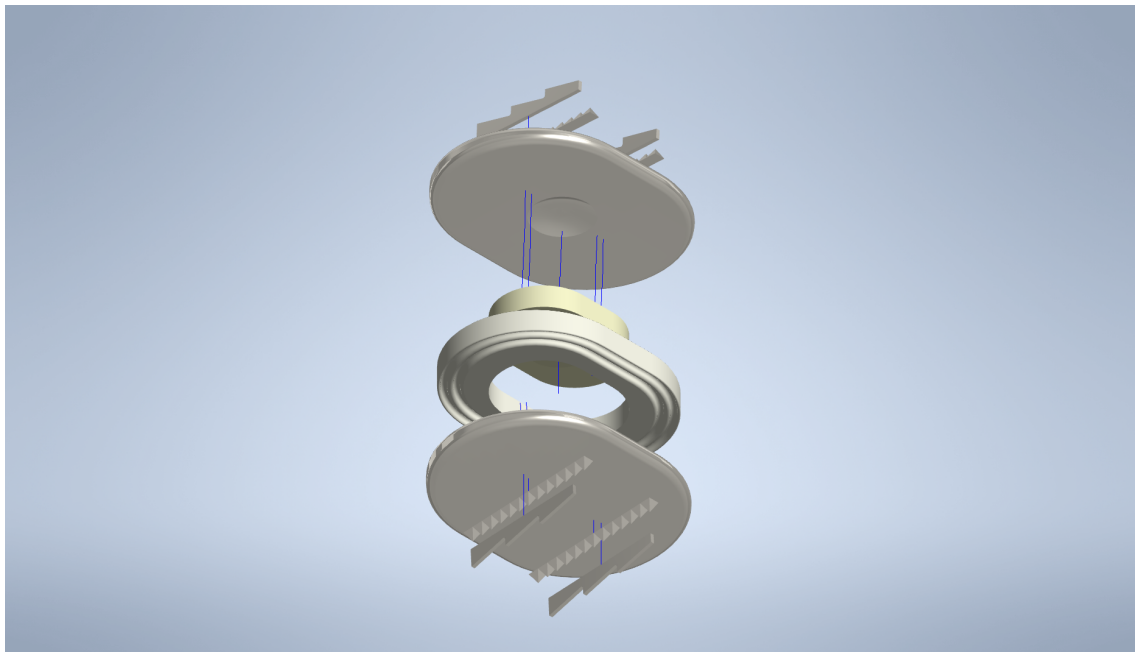


Figure 15: Exploded Side View

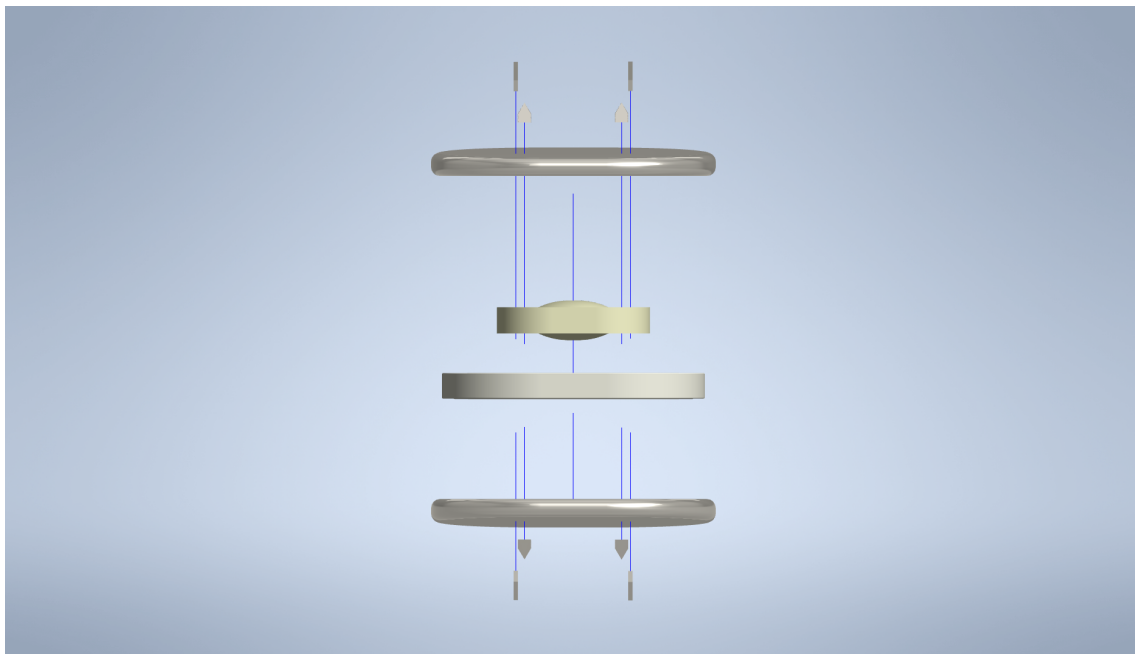


Figure 16: Summary of Maximum Stress Analysis Results

Result Summary

Name	Minimum	Maximum
Volume	41290.7 mm ³	
Mass	0.143464 kg	
Von Mises Stress	0.00000000189998 MPa	67.9859 MPa
1st Principal Stress	-3.19052 MPa	89.0941 MPa
3rd Principal Stress	-50.6344 MPa	25.7671 MPa
Displacement	0 mm	0.0114824 mm
Safety Factor	4.05378 ul	15 ul
Stress XX	-16.9772 MPa	45.0072 MPa
Stress XY	-22.8463 MPa	16.7128 MPa
Stress XZ	-8.98227 MPa	6.54316 MPa
Stress YY	-34.2959 MPa	49.0746 MPa
Stress YZ	-23.8095 MPa	29.2522 MPa
Stress ZZ	-28.3346 MPa	73.3428 MPa
X Displacement	-0.00185318 mm	0.00179763 mm
Y Displacement	-0.0114593 mm	0.0000012929 mm
Z Displacement	-0.00268076 mm	0.00258118 mm
Equivalent Strain	0.0000000000000000167681 ul	0.00256832 ul
1st Principal Strain	0.0000000000000000144507 ul	0.00204305 ul
3rd Principal Strain	-0.00239169 ul	0.0000139486 ul
Strain XX	-0.000377632 ul	0.000567311 ul
Strain XY	-0.000820522 ul	0.00102382 ul
Strain XZ	-0.000591596 ul	0.000549107 ul
Strain YY	-0.00198 ul	0.000562722 ul
Strain YZ	-0.00159365 ul	0.0013957 ul
Strain ZZ	-0.000424664 ul	0.0016245 ul
Contact Pressure	0 MPa	127.595 MPa
Contact Pressure X	-23.3463 MPa	40.4004 MPa
Contact Pressure Y	-111.124 MPa	68.7508 MPa
Contact Pressure Z	-47.9553 MPa	40.2574 MPa

Figure 17: Summary of Stress Analysis Results

Result Summary

Name	Minimum	Maximum
Volume	41290.7 mm ³	
Mass	0.143464 kg	
Von Mises Stress	0.000000000352216 MPa	12.7059 MPa
1st Principal Stress	-0.600197 MPa	16.7605 MPa
3rd Principal Stress	-9.48611 MPa	4.81979 MPa
Displacement	0 mm	0.00213706 mm
Safety Factor	15 ul	15 ul
Stress XX	-3.18795 MPa	8.41737 MPa
Stress XY	-4.27683 MPa	3.12926 MPa
Stress XZ	-1.69306 MPa	1.24228 MPa
Stress YY	-6.41685 MPa	9.18607 MPa
Stress YZ	-4.4438 MPa	5.49946 MPa
Stress ZZ	-5.29434 MPa	13.8009 MPa
X Displacement	-0.000342315 mm	0.000333916 mm
Y Displacement	-0.00213269 mm	0.000000200828 mm
Z Displacement	-0.000498002 mm	0.000478789 mm
Equivalent Strain	0.000000000000000310843 ul	0.000384798 ul
1st Principal Strain	-0.0000000000000760514 ul	0.000304446 ul
3rd Principal Strain	-0.000359745 ul	0.00000260236 ul
Strain XX	-0.0000509818 ul	0.000105748 ul
Strain XY	-0.000131494 ul	0.000101569 ul
Strain XZ	-0.0000835938 ul	0.0000916599 ul
Strain YY	-0.000317605 ul	0.0000824794 ul
Strain YZ	-0.000218635 ul	0.000258141 ul
Strain ZZ	-0.000093412 ul	0.000267915 ul
Contact Pressure	0 MPa	23.8346 MPa
Contact Pressure X	-4.37365 MPa	7.58614 MPa
Contact Pressure Y	-20.7872 MPa	12.8371 MPa
Contact Pressure Z	-8.85626 MPa	7.40337 MPa

Figure 18: Displacement Stress Analysis Results

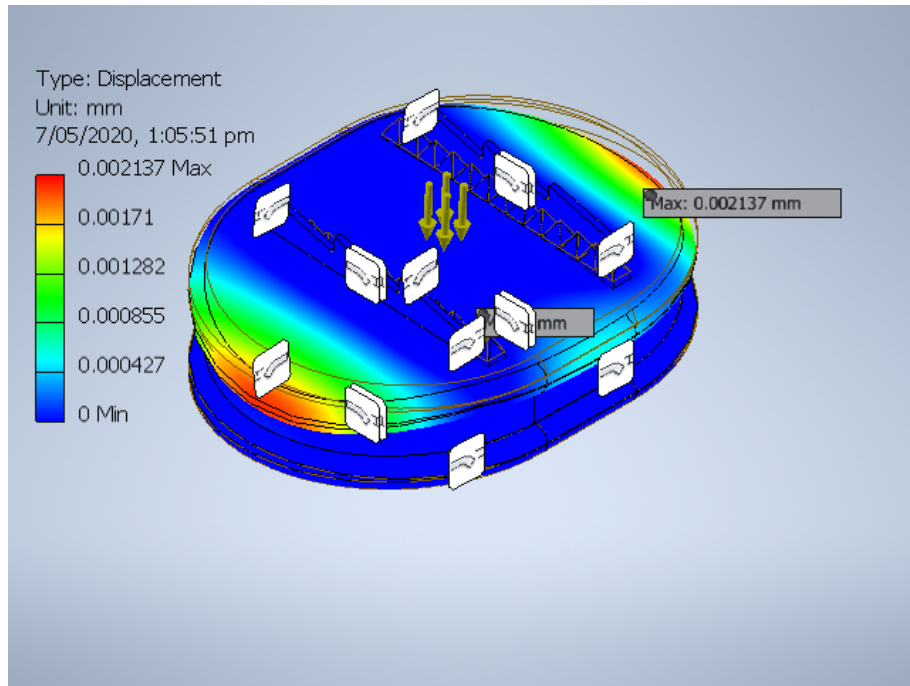


Figure 19: Strain Stress Analysis Results

